ACS APPLIED MATERIALS & INTERFACES

Research Article

www.acsami.org

Antibacterial Surgical Silk Sutures Using a High-Performance Slow-Release Carrier Coating System

Xiaojie Chen,[†] Dandan Hou,[†] Lu Wang,*[,†] Qian Zhang,[†] Jiahan Zou,[†] and Gang Sun[†,‡]

[†]Key Laboratory of Textile Science and Technology, Ministry of Education, College of Textiles, Donghua University, Songjiang District, Shanghai 201620, China

[‡]Division of Textiles and Clothing, University of California, Davis, California 95616, United States

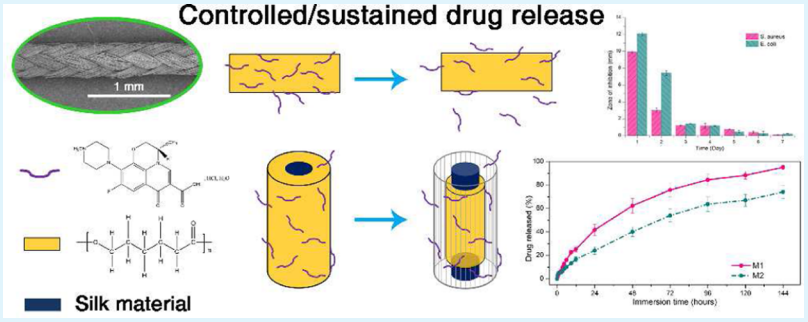

ABSTRACT: Sutures are a vital part for surgical operation, and suture-associated surgical site infections are an important issue of postoperative care. Antibacterial sutures have been proved to reduce challenging complications caused by bacterial infections. In recent decades, triclosan-free sutures have been on their way to commercialization. Alternative antibacterial substances are becoming relevant to processing surgical suture materials. Most of the antibacterial substances are loaded directly on sutures by dipping or coating methods. The aim of this study was to optimize novel antibacterial braided silk sutures based on levofloxacin hydrochloride and poly(ε-caprolactone) by two different processing sequences, to achieve suture materials with slow-release antibacterial efficacy and ideal physical and handling properties. Silk strands were processed into sutures on a circular braiding machine, and antibacterial treatment was introduced alternatively before or after braiding by two-dipping−two-rolling method (M1 group and M2 group). The antibacterial activity and durability against *Staphylococcus aureus* and *Escherichia coli* were tested. Drug release profiles were measured in phosphate buffer with different pH values, and release kinetics model was built to analyze the sustained drug release mechanism between the interface of biomaterials and the *in vitro* aqueous environment. Knot-pull tensile strength, thread-to-thread friction, and bending stiffness were determined to evaluate physical and handling properties of sutures. All coated sutures showed continuous antibacterial efficacy and slow drug release features for more than 5 days. Besides, treated sutures fulfilled U.S. Pharmacopoeia required knot-pull tensile strength. The thread-to-thread friction and bending stiffness for the M1 group changed slightly when compared with those of uncoated ones. However, physical and handling characteristics of the M2 group tend to approach those of monofilament ones. The novel suture showed acceptable *in vitro* cytotoxicity according to ISO 10993-5. Generally speaking, all coated sutures show potential in acting as antibacterial suture materials, and M1 group is proved to have a higher prospect for clinical applications.

KEYWORDS: *surgical silk suture, antibacterial properties, coating, controlled release/sustained release, physical and handling characteristics*

INTRODUCTION

Surgical site infections (SSIs) are challenging surgical complications occurring after surgical procedures. Based on the surveillance system of the Centers for Disease Control and Prevention (CDC), SSIs were the third most common nosocomial infection (17%) among hospitalized patients.[1,2] In 2011, the conservative estimated number of SSIs was 157,500 (21.8%) among major types of health-care-associated infections in the United States.[3] More than that, SSIs prolonged the length of stay in hospitals by 9.7 days, while adding extra cost by $20,842 per admission,[4] and were also a significant cause of postoperative mortality.[5]

One of multitudinous surgical risk factors for SSIs is suture materials, especially braided sutures and suture knots.[6] As a foreign body, suture materials have the potential of bacteria bioadherence and lead to accumulation of microbial colonization on surgical incisions. Microorganisms colonize the suture and then proliferate to form an adherent biofilm. Once the biofilm is established, the risk of SSIs is higher, and elimination of the micropopulation is more difficult.[6,7] Braided silk sutures have a higher risk of SSIs because their protein

Received: July 10, 2015
Accepted: September 17, 2015
Published: September 17, 2015

DOI: 10.1021/acsami.5b06239
ACS Appl. Mater. Interfaces 2015, 7, 22394−22403

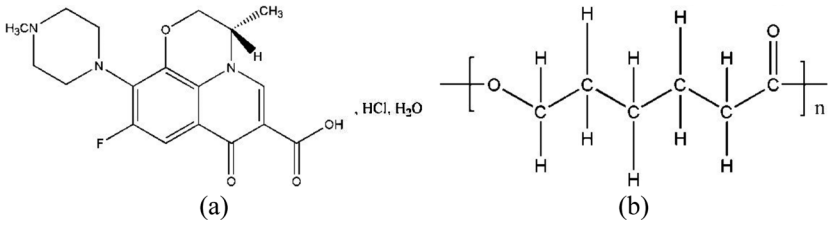

Figure 1. Total or partial chemical structures of (a) levofloxacin hydrochloride (LVFX-HCl) and (b) poly(ε-caprolactone) (PCL).

nature easily attaches to bacteria and the braided structure easily hides bacteria. A report in 1957 showed that a sterile silk suture could enhance the development of infection up to 10,000-fold *in vivo*.[8,9]

Alexander et al.[8] pointed out that suture materials with antibacterial treatment showed the feasibility of inhibiting bacterial growth in wounds and reducing the infection rate. Triclosan-impregnated Polyglactin 910 (Vicryl Plus, Ethicon Inc., Somerville, NJ, USA), which received approval from the Food and Drug Administration in 2002,[6] is one of the commercial demonstrations. Nevertheless, the wide nonmedical use of triclosan may contribute to potential selection of bacteria and triclosan-adapted cross-resistance with antibiotics.[10,11] Moreover, a potential of wound breakdown with triclosan-combined sutures in breast reduction surgery has been reported.[6]

Therefore, new alternative substances have been employed, such as chlorhexidine, sulfamethoxazole trimethoprim, tetracycline hydrochloride, and levofloxacin.[12−15] All these substitutions demonstrated high antibacterial efficacy.

Silk sutures possess excellent physical and handling properties, such as ease of knotting and good knot security,[16,17] which is a generally recognized clinical experience. However, any antibacterial treatment, especially with polymer coating, may adversely affect these properties. Thus, fabrications and modifications of silk suture materials should be optimized and their distinguished physical and handling properties should be retained.

The objective of this present work was to optimize a novel formulation of braided silk suture materials coated with an antibacterial mixture of levofloxacin hydrochloride (LVFX-HCl) and poly(ε-caprolactone) (PCL). Two different coating processes were used, and antibacterial efficacy and ideal slow drug release features were achieved on the treated silk sutures. Besides, the release kinetics model was established and the sustained drug release mechanism between the interfaces of the novel suture materials and aqueous environments with different pH values was analyzed. Physical and handling characteristics, including knot-pull tensile strength, thread-to-thread friction, and bending stiffness, were measured. The U.S. Pharmacopoeia required knot-pull tensile strength was reached by all samples. Nevertheless, obvious differences of thread-to-thread friction and bending stiffness were observed because of different process sequences. We conducted these investigations to make a useful attempt for clinical applications of novel antibacterial braided silk suture materials.

MATERIALS AND METHODS

Raw Materials for Surgical Sutures. Silk strands (Nantong Horcon Medical Technology Co., Ltd., Haimen, China), with two different finenesses (60 D for shell strand and 140 D for core strand), were used for preparation of the antibacterial sutures.

Antibacterial Coating Solution. Antibacterial coating solution was prepared by dissolving poly(ε-caprolactone) (PCL, M_w = 180,000 g/mol, Shenzhen BrightChina Industrial Co., Ltd., Shenzhen, China) and levofloxacin hydrochloride (LVFX-HCl, Jiangsu Xiangrui Pharmaceutical Co., Ltd., Yancheng, China) in 99.5% acetic acid (Sinopharm Chemical Reagent Co., Ltd., Beijing, China) (Figure 1). The mass content of PCL in the solution system was 5% (w/w), and the concentration of LVFX-HCl in the coating solution was maintained at 3000 μg/mL.

Preparation of Antibacterial Sutures. A normal circular braiding machine (Figure 2) with the cogwheel ratio adjusted to

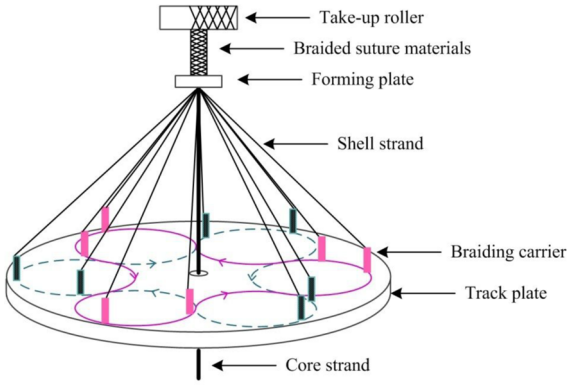

Figure 2. Schematic drawing of a normal circular braiding machine.

130/36 was used to produce braided silk sutures. Each braided silk suture was composed of 12 shell strands and 1 core strand. Twelve carriers carried 12 pieces of shell strands to realize independent, continuous motion around the static core strand placed in the middle on the circular braiding machine. The antibacterial treatments were designed to alternate before or after the braiding process.

Both shell and core strands were treated with the antibacterial coating solution by passing through a two-dipping−two-rolling coating machine (Figure 3). Then after drying, the strands were braided by the circular braiding machine to prepare antibacterial sutures (method 1). Coating repetitions of the strands were applied once, twice, and thrice, expressed as M1-1, M1-2, and M1-3, respectively.

Alternatively, the strands were previously braided by the circular braiding machine to become yarns. Then, the braided yarns were charged with the antibacterial coating system by the same two-dipping−two-rolling coating machine (method 2). Coating repetitions of the braided yarns were conducted once, twice, and thrice, expressed as M2-1, M2-2, and M2-3, respectively.

Uncoated braided silk sutures in the same braided parameter were used as a reference, which were expressed as R. The samples of PCL-coated sutures without containing LVFX-HCl were also fabricated as a reference for antibacterial assays and *in vitro* cytotoxicity testing.

Surface Morphology of Antibacterial Sutures. SEM images of sutures with and without antibacterial treatment were obtained using the scanning electron microscope SU8000 (Hitachi, Tokyo, Japan). The SEM images of antibacterial sutures exposed to *Staphylococcus aureus* (*S. aureus*, ATCC 25923) and *Escherichia coli* (*E. coli*, ATCC 25922) were compared with SEM images of the sutures without antibacterial agent. The samples were placed in bacterial suspensions

DOI: 10.1021/acsami.5b06239
ACS Appl. Mater. Interfaces 2015, 7, 22394−22403

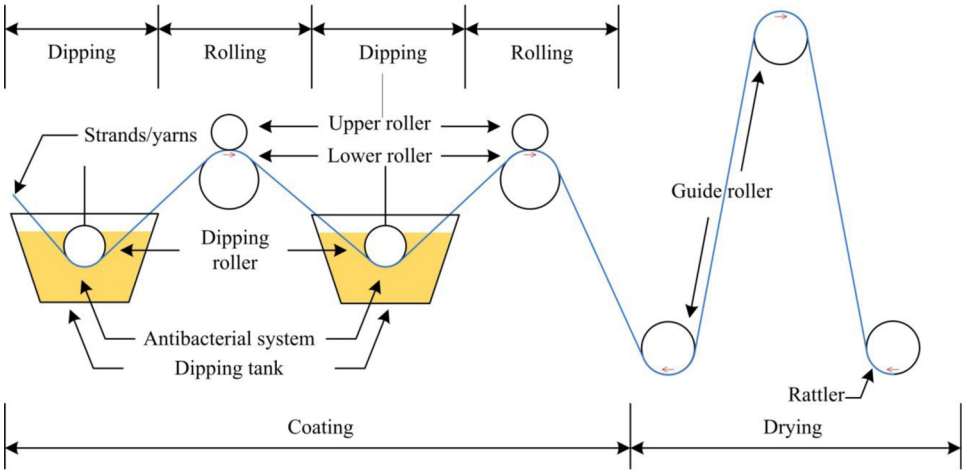

Figure 3. Schematic drawing of a two-dipping–two-rolling coating machine.

with the concentration of 1×10^5 colony forming units/mL (CFU/mL) and incubated at 37 °C for 24 h. After incubation, the sutures were first washed by phosphate buffered solution (PBS, pH = 7.2), and then immersed in 10% formaldehyde solution at 4 °C for 30 min. At the end, samples were washed with 75% alcohol and then washed again with 100% alcohol to remove water.

The difference of weight change before and after antibacterial coating was estimated as weight per unit length. This assay was carried out on sutures of 5 cm in length. An electronic analytical balance (TP-114, Denver Instrument (Beijing) Co., Ltd., Beijing, China) was used to weight each sample.

The diameter of individual sutures was determined according to the U.S. Pharmacopeia 37.[18] An electronic dead-weight thickness gauge (CH-10-AT, Shanghai Liuling Instrument Factory, Shanghai, China) was used to measure the diameters. The diameters of the samples were measured at 10 different positions along the length of the suture. For each test point, two measurements were tested at right angles to each other.

Antibacterial Activity. *a. Qualitative Assay—Agar Diffusion Plate Test.* The sensitivity of the organism to the antibacterial agent is judged by the zone of inhibition.[19] This assay was carried out on silk sutures of 5 cm in length. Pieces of samples were inoculated with approximately 1 mL of bacterial suspension (1×10^8 CFU/mL) per tryptic soya agar plate. The plates were incubated at 37 °C for 24 h and then measured by a digital vernier caliper to determine the zone of inhibition around the suture (Figure 4). Gram-positive *S. aureus* and

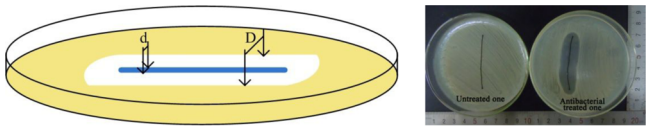

(a) (b)

Figure 4. Zones of inhibition: (a) schematic drawing; (b) photograph.

Gram-negative *E. coli* were selected as the testing organisms. The assessments were performed according to antibacterial activity evaluation standard (ISO 20645:2004). In this assay, the samples of PCL-coated sutures without containing LVFX-HCl were tested as a reference.

Note: The zone of inhibition is calculated according to the following formula,

$$H = (D - d)/2$$

where H = the zone of inhibition (mm), D = the total diameter of the specimen and the zone of inhibition (mm), and d = the diameter of the specimen (mm).

b. Sustained Efficacy Assay—Serial Plate Transfer Test. The purpose of this assay was to determine the duration of antibacterial activity of the coated sutures. Suture samples were transferred onto new Petri dishes inoculated with similar numbers of bacteria.[15,20] The test was continued until the sutures ceased antibacterial functions.

Release Kinetics of the Antibacterial Agent. The release characteristics of LVFX-HCl from the antibacterial sutures were measured in an aqueous environment to simulate the drug release during usage. Threads (60 cm) were placed in centrifuge tubes with the release medium (8 mL) at 37 °C on a shaker with a shaking speed of 60 rpm. The release mediums were buffer solutions with three different pH values, pH 6.3, pH 6.8, and pH 7.7, which corresponded to three skin pH values of the relative lower, normal, and relative higher points[21] during wound healing. Buffer solutions (Table 1) were

Table 1. Formula of Release Media with Different pH Values (100 mL)[a]

pH value	solution A (mL)	solution B (mL)
6.3	77.5	22.5
6.8	51.0	49.0
7.7	10.5	89.5

[a]Solution A, 0.2 mol/L NaH_2PO_4; solution B, 0.2 mol/L Na_2HPO_4.

made from sodium dihydrogen phosphate dihydrate ($NaH_2PO_4 \cdot 2H_2O$, analytical reagent) and disodium hydrogen phosphate dodecahydrate ($Na_2HPO_4 \cdot 12H_2O$, analytical reagent). At procedural time points, a 1 mL solution of each sample was extracted to measure the absorption intensity of LVFX-HCl by using a UV–vis spectra photometer (TU-1901, Beijing Purkinje General Instrument Co., Ltd., Beijing, China) at the maximal absorption peak with wavelengths of 290 nm (pH 6.3), 289 nm (pH 6.8), and 287 nm (pH 7.7), which are the corresponding wavelengths (290 nm for pH 6.3, 289 nm for pH 6.8, and 287 nm for pH 7.7) of the maximum peak values of absorption intensity for a series of drug solutions under the corresponding pH values. Meanwhile, an equal amount of fresh buffer was supplemented to each centrifuge tube. The accumulative release rate (%) was calculated as the ratio of drug release amount at each procedural time point to the amount of drug loaded on the threads.

***In Vitro* Cytotoxicity Test.** The cytotoxicity test of R, M1-2, and a commercial surgical silk suture as reference were evaluated according to ISO 10993-5:2009. The evaluation was performed by measuring the viabilities of the cells according to liquid extract test method. Porcine endothelial cells (PIECs, Keygen Biotechnology Co.) were cultivated in Dulbecco's modified Eagle medium (DMEM, Gibco) containing 10% fetal bovine serum (Gibco) at 37 °C and 5.0% CO_2. The extract of material was generated by immersing the coated samples (0.05 g) in 1 mL of DMEM for 24 h at 37 °C. Simultaneously, 100 μL of cell

DOI: 10.1021/acsami.5b06239
ACS Appl. Mater. Interfaces 2015, 7, 22394–22403

medium incubated as 4000 cells/well inside 96 well plates for 4 h. Then, the cell medium was swapped with 100 μL extracts to additional culture of 20 h. Finally, cell counting kit-8 (CCK-8, 10 μL) was added, and the optical density value was measured by a microplate reader (Multiskan FC, Thermo) at 450 nm after 4 h. The viability of pure PIECs culture not containing any sample was tested as blank. The reduction of cell viability by more than 30% is considered as cytotoxic effect according to ISO 10993-5:2009.[22] In this assay, the samples of PCL-coated sutures without containing LVFX-HCl were introduced as a reference.

Mechanical Properties and Handling Characteristics. *a. Knot-Pull Tensile Strength.* YG (B) 026G-500 universal testing system instrument (Wenzhou Darong Textile Instrument Co., Ltd., Wenzhou, China) was used for tensile strength tests. The testing parameters of the knot-pull tensile strength of each individual suture were determined according to the U.S. Pharmacopeia 37.[18] A simple knot was used in this test.

b. Thread-to-Thread Friction. Thread-to-thread friction was measured by using a XF-1A surgical suture friction tester (Shanghai New Fiber Instrument Co., Ltd., Shanghai, China). Three of the same sutures of 15 cm in length were prepared, and each was hanged with a weight of 20 cN. Two samples were entwined horizontally to make sure the other sample pulled up vertically through the crossed space of them.[16] The dragging speed of the vertical one was 75 mm/min. The friction force during the whole movement of the vertical one was recorded, and both maximum static friction and average dynamic friction were reported from the friction force curve.

c. Bending Stiffness. Sutures of 5 cm in length were placed horizontally. Then 1 cm of either end which attached to the weight was hanged in midair. After 15 s, the distance between the level of the suture and the bending end was measured. The bending stiffness was then calculated by the equation of the cantilever beam law.[23]

Statistical Analysis. The statistical analyses were performed using the student's *t* test (SPSS 19.0) with significant level $p < 0.05$. The data reported were the means and standard deviations, and the error bars in the figures correspond to one standard deviation. The data in the figures were marked by an asterisk (*) for $p < 0.05$ and double asterisks (**) for $p < 0.01$.

RESULTS

Surface Morphology of Coated Sutures. The surfaces of the silk suture materials (Table 2) without antibacterial treatment were a little disordered. However, strands of antibacterial sutures arranged in order. M1-2 maintained the braided structure more clearly, while the space of crossed strands of M2-2 filled with the antibacterial coating.

Table 2. SEM Images of Sutures with Different Treating Methods

R	M1-2	M2-2
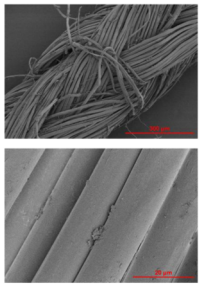	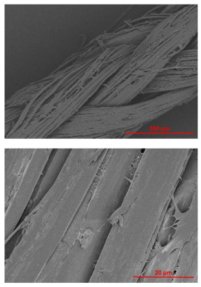	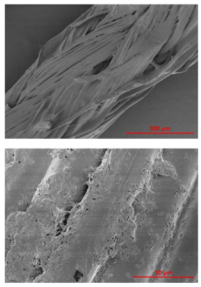

The changes of weight ($n = 5$) and diameter ($n = 10$) of sutures with different treating parameters are shown in Figure 5. For both M1 and M2 groups, the total weights increased with repeated coating process, but the weight values of M2 group samples were much closer. As antibacterial treatment was applied, the average diameters of both groups increased to varied degrees. However, a declining trend was observed for M1-3.

Antibacterial Activity. When uncoated silk sutures were exposed to *S. aureus* and *E. coli* (Table 3), the suture surfaces were heavily covered with bacteria cells. In addition, bacteria easily hid between the interstices of the strands, which were protected from phagocytosis by leukocytes.[8,24] The SEM images of the coated sutures showed almost no bacteria attachment, which could potentially reduce the risk of forming a biofilm on the surfaces.

Coated sutures (M1 group) revealed *S. aureus* inhibition zones after incubation for 24 h of 9.19 mm (M1-1), 11.48 mm (M1-2), and 10.38 mm (M1-3), and *E. coli* inhibition zones of 11.39 mm (M1-1), 12.07 mm (M1-2), and 11.24 mm (M1-3), respectively. For both types of bacteria (Figure 6), the inhibition zones decreased rapidly during the first 3 days. Then the zones of inhibition changed in a stable trend. The durations of inhibition zones were maintained varying from 5 to 7 days. M1-1 and M1-2 ended up after 5 (*S. aureus*) or 6 days (*E. coli*) of experiments, whereas M1-3 lost the function after 7 days. The results of inhibition zones and durations of the M2 group were similar. Meanwhile, the zones of inhibition for two types of bacteria showed a difference in the first day. Inhibition zones against *S. aureus* were measured as 9.39 mm (M2-1), 9.72 mm (M2-2), and 9.93 mm (M2-3), and 11.70 mm (M2-1), 11.35 mm (M2-2), and 12.08 mm (M2-3) against *E. coli*, respectively. Sutures coated with PCL without containing LVFX-HCl showed no zones of inhibition.

Release Kinetics of Antibacterial Agent from Coated Sutures. All coated samples demonstrated continuous drug release within 5−6 days of experiments (Figure 7, Figure 8). The initial burst period of drug release was observed during the first 12 h, and the amount of the drug released remained stable after 96 h. LVFX-HCl was continuously released from sutures resulting in total drug released proportions of 94.56% (M1-1), 95.02% (M1-2), and 88.32% (M1-3), respectively (Figure 7). The total drug release ratios of M2 group samples reached less than 80%, which were 79.19% (M2-1), 74.13% (M2-2), and 83.21% (M2-3), respectively (Figure 7). Overall, the drug release rate of the M1 group at each procedural time point was higher than that of the M2 group (Figure 7). In addition, the drug release rate in alkaline environment was faster than that in acidic environment, and the total drug release ratios were 12−15% higher in alkaline environment (Figure 8).

***In Vitro* Drug Cytotoxicity.** The CCK-8 assay ($n = 3$) results are shown in Figure 9, revealing a decrease of cell viability after antibacterial treatment compared with the results of the commercial ones. The viabilities ended with the absorbance at 0.849 (blank), 0.816 (commercial silk suture), 0.753 (R), 0.781 (PCL only), and 0.681 (M1-2), respectively.

Knot-Pull Tensile Strength of Sutures. The mean knot-pull tensile strength values ($n = 5$) of all sutures (Figure 10) tested demonstrated higher values than 10.0 and 14.2 N for class II nonabsorbable surgical suture at size 2-0 and size 0, respectively, the required strength by the USP 37. However, the knot-pull tensile strength values of the M2 group showed a significant decrease with more coatings. Moreover, when considering the increase of suture diameters, a conversion of intensity of knot-pull tensile strength was obtained. All of the intensity values declined, especially the values of the M2 group samples showed a huge fall compared to R (values in

DOI: 10.1021/acsami.5b06239
ACS Appl. Mater. Interfaces 2015, 7, 22394−22403

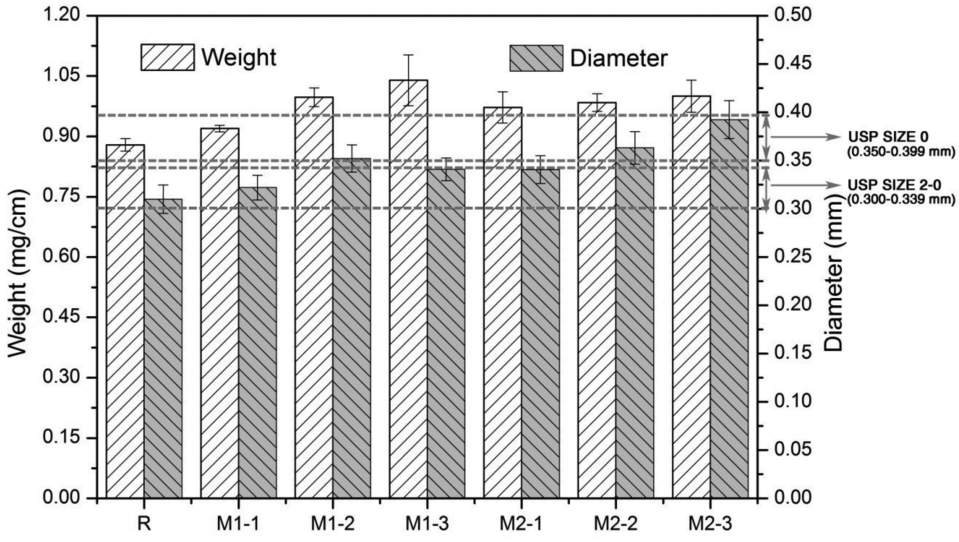

Figure 5. Weight and diameter changes of sutures with different treating methods.

Table 3. SEM Images of the Surface of the Untreated (R) and Antibacterially Treated (M1-2) Sutures

	Sutures exposed to *S. aureus*	Sutures exposed to *E. coli*
Untreated sutures (*R*)	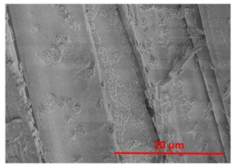	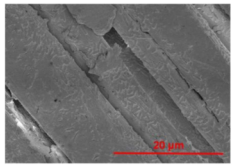
Antibacterial treated sutures (*M1-2*)	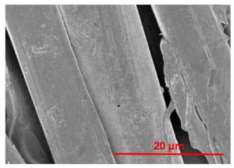	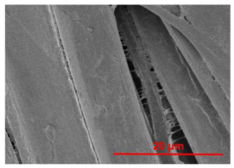

megapascals declined by up to 35%) and the M1 group (values in megapascals declined by about 25−30%).

Thread-to-Thread Friction of Sutures. The maximum static resistance and average dynamic resistance of all of the samples are indicated in Figure 11 (n = 5). Both of these two resistance values increased for the M1 group, which were not only increased with the repetitions of coating, but also higher than those of R. On the contrary, the resistance results revealed a moderate drop with added coating times for the M2 group, which are also accounted for at about half of that of R.

The D-value was defined as the difference between the maximum static and average dynamic friction resistances. The D-value narrowed for the M1 group, while it enlarged for the M2 group (Figure 12).

Bending Stiffness of Sutures. The average bending stiffness (n = 5) of sutures (Table 4) changed significantly

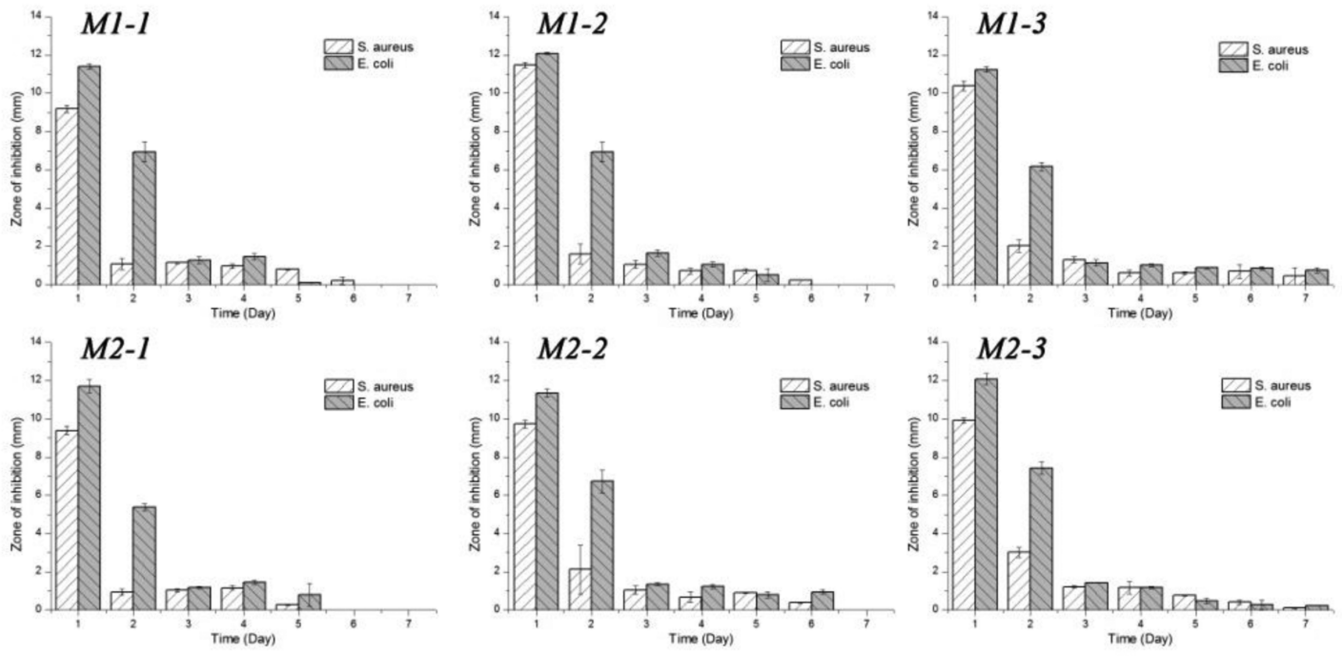

Figure 6. Sustained antibacterial efficacy assay of sutures with different treating methods (n = 5).

DOI: 10.1021/acsami.5b06239
ACS Appl. Mater. Interfaces 2015, 7, 22394−22403

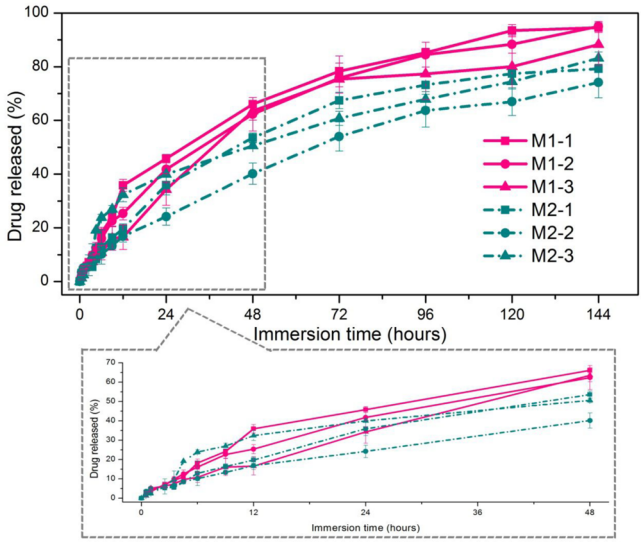

Figure 7. Drug release curves of coated sutures at pH 6.8 (n = 3).

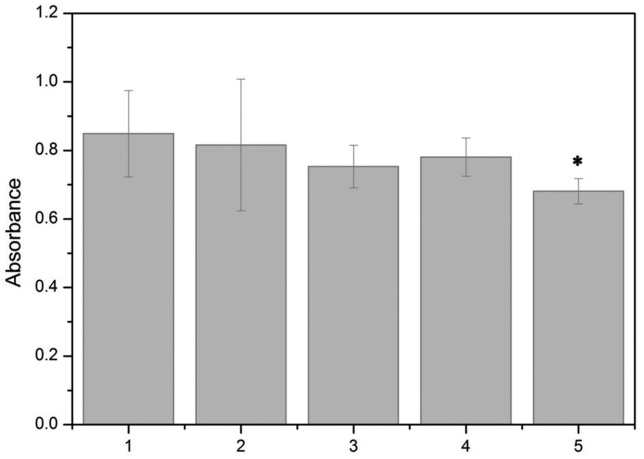

Figure 9. Cytotoxicity assays of the (1) blank, (2) commercial silk suture, (3) R, (4) PCL only, and (5) M1-2. Significant differences were marked by an asterisk (*) for $p < 0.05$ compared with the blank.

because of the changed preparation processes and the increased coating time. The bending stiffness value of M2-3 shot up 10-fold compared to that of R. However, the bending stiffness values of the M1 group approximately doubled compared to that of R.

DISCUSSION

As a foreign material, sutures can cause device-related SSIs by adhering pathogens and proliferating to form infamous biofilms. Antibacterial suture materials can effectively inhibit bacterial growth, prevent formation of biofilms, and reduce the infection. Some literature has proved or agreed with the effects of antibacterial sutures to defeat SSIs.

The disordered surface of untreated silk sutures was related to the rubbing and drafting of the circular braiding machine.

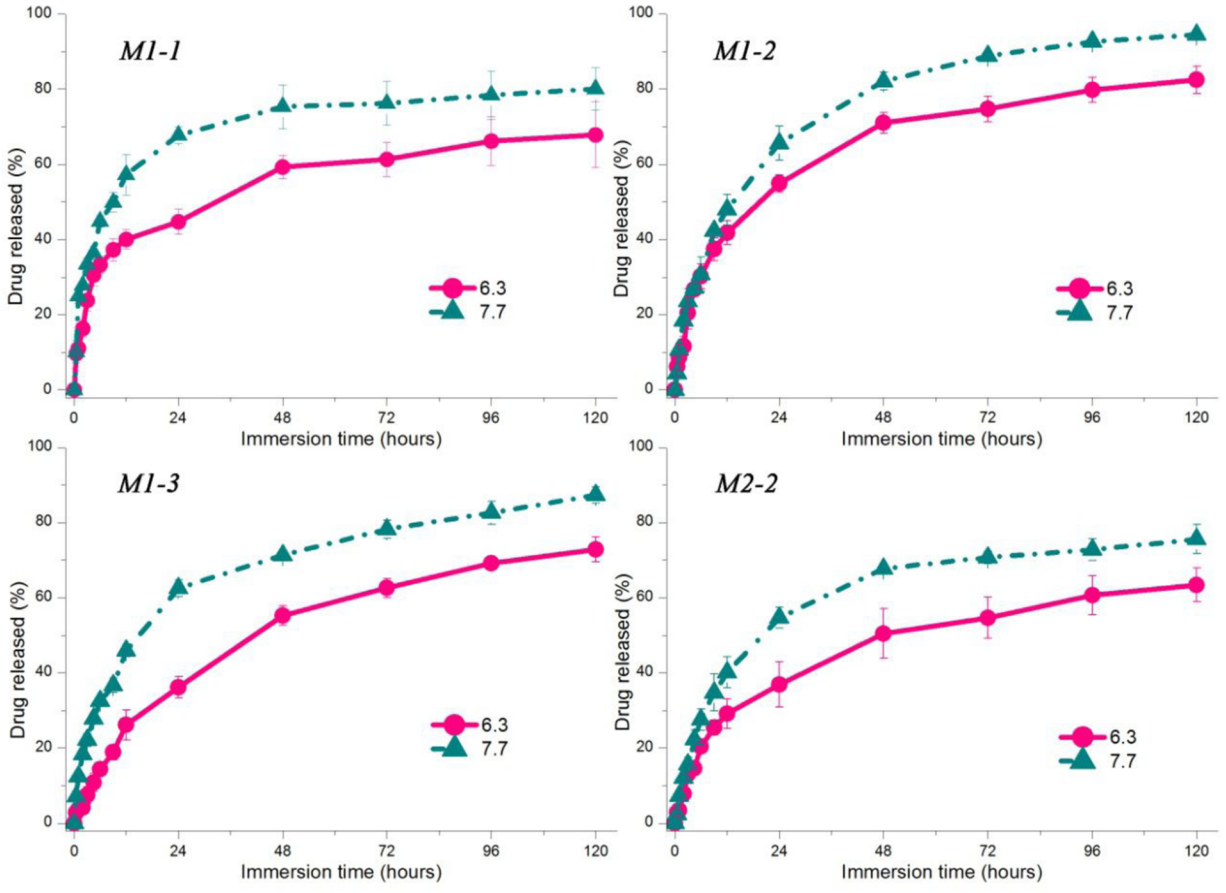

Figure 8. Drug release analysis of coated sutures at pH 6.3 and pH 7.7 (n = 3).

DOI: 10.1021/acsami.5b06239
ACS Appl. Mater. Interfaces 2015, 7, 22394−22403

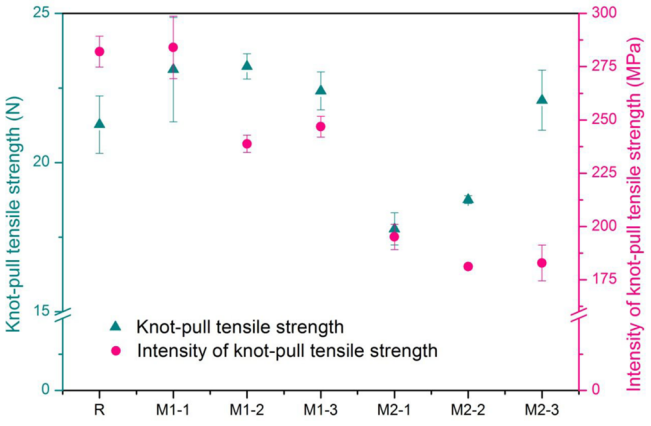

Figure 10. Knot-pull tensile strength of sutures with different treating parameters.

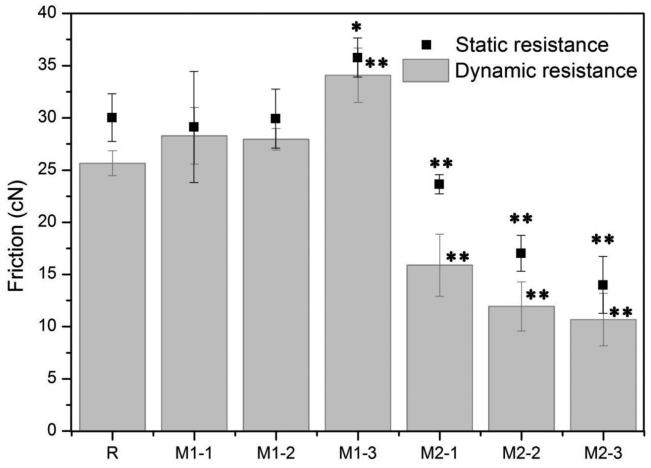

Figure 11. Thread-to-thread friction of sutures with different treating parameters. Significant differences were marked by a single asterisk (*) for $p < 0.05$ and double asterisks (**) for $p < 0.01$ compared with R.

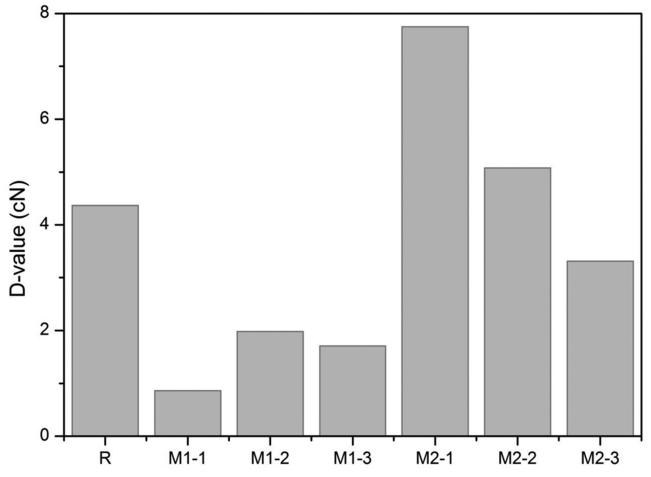

Figure 12. Difference between static and dynamic friction resistances of each sample (*D*-value = the mean of maximum static friction for each sample in Figure 11 − the mean of average dynamic friction for the corresponding sample in Figure 11).

However, antibacterial coating acted as protection during the manufacture by wearing a thin film outside the strands or sutures. The braided structure and surface irregularity of the M2 group was not obvious; the appearances and mechanical properties might tend to approach the performance of monofilament suture.

The weight of the coated sutures increased with varying degrees. In practical terms, that increase was more apparent for the M1 group compared to the M2 group, caused by the M2 series preventing more coating materials from permeating into gaps between the braided strands after the first coating.

The pattern of diameter change almost matched that of weight, except that a downtrend was observed in the M1 group after the suture was coated twice. The downtrend was caused by the pressure of rollers in the two-dipping−two-rolling procedure (Figure 3). The strands or sutures will be always covered with antibacterial solution after passing through a container filled with the antibacterial mixture. Then the draw-off mechanism guided strands or sutures to go across from the middle of two vertical rollers (Figure 13a). The distance of the two rollers was adjusted by a mechanical spring, controlling the coating thickness and applying pressure on threads to encourage more antibacterial coating to permeate into the inner space (Figure 13b). As the fineness of the strands increased for method 1, the unaltered roller-to-roller distance resulted in difficulties for extra antibacterial cover being maintained on the surface of the strands because of less space and even caused deformation of strands and sutures by overlarge pressure such as M1-3 (for the M2 group, a pressure-free method was used). Thus, the coherence between roller-to-roller distance and increased coating repetitions deserves more effort.

In both the zone of inhibition assay and the sustained efficacy assay, braided silk sutures with LVFX-HCl demonstrated efficacy *in vitro* against Gram-positive and Gram-negative isolates. However, *E. coli* is more susceptible to LVFX-HCl *in vitro* than *S. aureus* (Figure 6).[25]

Data in Figure 6 describe a sustained efficacy of LVFX-HCl spanning up to 7 days. Corresponding to this profile, continuous drug release within 5−6 days was measured for antibacterial braided sutures. Sustained antibacterial efficacy of braided silk sutures is a desirable characteristic because it continuously provides protection to surgical incision against bacterial growth before the rebuilding of anatomic barriers and the complete healing of a wound.[26] In general, antibacterial suture inhibits bacterial colonization. Meanwhile, as the antibacterial drug diffuses away from the implant, a concentration gradient of antibacterial drug in the aqueous environment is formed. Therefore, antibacterial braided silk suture becomes a useful approach for postoperative prophylactic management against device-related SSIs.

The release rate constants of all of the drug-carried samples were calculated from the drug release experimental results at both pH 6.3 and pH 7.7 (Figure 8) according to different theoretical models.

zero-order model:

$$M_t/M_\infty = kt$$

first-order model:

$$\ln(1 - M_t/M_\infty) = -kt$$

Higuchi model:

$$M_t/M_\infty = kt^{1/2}$$

DOI: 10.1021/acsami.5b06239
ACS Appl. Mater. Interfaces 2015, 7, 22394−22403

Table 4. Bending Stiffness (cN/mm^2) of Sutures with Different Treating Parameters

R	M1-1	M1-2	M1-3	M2-1	M2-2	M2-3
1.48 ± 0.25	1.98 ± 0.58	2.81 ± 0.40	4.14 ± 1.75	8.02 ± 0.93	8.86 ± 2.97	14.19 ± 3.07

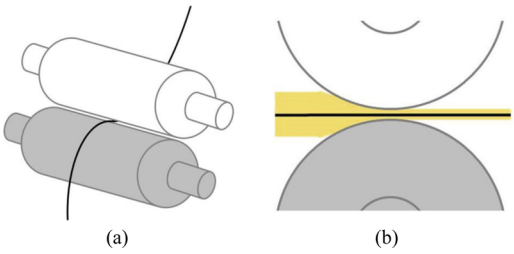

Figure 13. Illustration of rollers for two-dipping−two-rolling procedure: (a) overall graph (upper roller is plastic material; lower roller is metal material); (b) partial effect diagram during the coating process.

where M_t is the accumulated amount of drug released at time t, M_∞ is the total amount of drug on the suture sample, and M_t/M_∞ is the drug release ratio at time t, k is the release rate constant. The drug release ratios for the initial 12 h and their corresponding extracting time points are cited to fit to the preceding three mathematical models. Two parameters, release rate constants (k) and correlation coefficients (R), are obtained. The mathematical model with maximization of R and the minimization of mean square error (MSE) is the optimized mathematical model.

For drug-carried sutures (Table 5), the correlation coefficients for the Higuchi model were the highest. Therefore, we confirmed that the Higuchi model was the main mathematical hypothesis for the slow releasing of the drug from the suture materials. In addition, the square difference of the tested drug release ratio and fitted value according to the preceding fitting equations was smaller for the first-order model. Therefore, we predicted that the first-order model also influenced the drug delivery. To sum up, the combination of diffusion of drug in aqueous medium and the hydrolytic degradation of dosage decided the drug release from the antibacterial system.[27−29]

With the preceding theoretical analysis, the results of Figure 7 and Figure 8 can be explained here. Figure 7 shows that the drug release rate of the M1 group was about 10% quicker than others because the retained braided structure promoted the contact of coating film and the aqueous medium, which was indirectly conducive to drug diffusion. Figure 8 demonstrates that the alkaline environment accelerated the hydrolytic degradation. PCL undergoes the hydrolytic cleavage of ester groups at the original degradation.[30] The carboxylic end group byproducts build an acidic gradient in the aqueous medium. These acid byproducts could be neutralized in the basic environment, which in return could promote hydrolytic degradation of PCL and drug release from the PCL-based antibacterial system.

The initial burst period, caused by rapid released of the surface accumulation drug, is an unpredictable and uncontrollable factor for a long-term controlled release system.[31] Exploration on the prevention of the initial burst period deserves more effort.

The cytotoxicity is a key issue for biological applications of implantations. The ISO 10993 standard defines that a cytotoxic effect is determined quantitatively by the reserve of cell viability falling lower than 70%.[22] For the prepared samples, the viabilities were 96.11% (commercial silk suture), 88.69% (R), 92.00% (PCL only), and 80.21% (M1-2), respectively, indicating that no obvious cytotoxic effect existed for these tested items. However, the lower the viability value, the higher the cytotoxic potential of the test specimen was. Thus, the viabilities of laboratorial ones were a little more unsatisfactory than commercial ones. Kundu et al.[32] reported that coexistence of both silk protein fibroin and sericin might trigger macrophage-mediated inflammation. Altman et al.[33] reported the sericin glue-like proteins in silk materials have an adverse impact to biocompatibility and hypersensitivity. Shen et al.[34] demonstrated that silk fibroin fabric showed great toxicity because complete removal of sericin was not always ensured for the degummed fibroin. Some literature has verified that the process and combination of PCL would cause scarcely any cytotoxic potential to biomedical materials and tissue engineering,[35,36] which was also proved in Figure 9. On the contrary, the cell viability might increase with the existence of PCL. Hence, the decrease of the viability for M1-2 was possibly caused by the initial burst release resulting in a higher local drug concentration. Besides, the residual acetic acid could also affect the results. Therefore, more evaluations are needed on any new antibacterial sutures, at least for showing results comparable to the commercial ones.

All coated sutures prepared by the two-dipping−two-coating process showed higher average knot-pull tensile strength than the requirements set forth by the USP standard. Knot-pull tensile strength of the M1 group was negligibly influenced by the two-dipping−two-coating process, while that of the M2 group coated sutures displayed a noticeable drop. The PCL-based coating might not provide much contribution due to the fact that PCL lacks high mechanical properties for applications

Table 5. Release Rate Constants (k) and Correlation Coefficients (R) for the Fitting to Three Mathematical Models of the Drug Release from Coated Sutures

		M1-1		M1-2		M1-3		M2-2	
pH value	model	k	R	k	R	k	R	k	R
6.3	zero order	0.027	0.933	0.032	0.967	0.020	0.997	0.024	0.977
	first order	0.016	0.949	0.019	0.980	0.010	0.996	0.012	0.985
	Higuchi	0.121	0.979	0.138	0.992	0.084	0.976	0.102	0.994
7.7	zero order	0.035	0.942	0.036	0.972	0.031	0.973	0.032	0.979
	first order	0.025	0.973	0.022	0.988	0.019	0.986	0.018	0.991
	Higuchi	0.154	0.978	0.153	0.995	0.134	0.996	0.138	0.999

DOI: 10.1021/acsami.5b06239
ACS Appl. Mater. Interfaces 2015, 7, 22394−22403

requiring high load bearing.[37] Oppositely, an undesirable negative influence was accumulated during the two-dipping−two-coating process, because of the sustaining pressure transmitted to the strands and yarns by the self-weight of the rollers and rubbing of the draw-off mechanism. Consequently, the intensity of knot-pull tensile strength of almost all of the coated sutures decreased at different extents.

As mentioned earlier, the braided feature and surface irregularity of the M2 group was not apparent, the appearance was similar to both monofilament sutures and multifilament braided sutures. Furthermore, the mechanical properties, especially thread-to-thread friction and bending stiffness of the M2 samples, showed some tendency close to the characteristics of monofilament sutures.

The knot holding capacity and ease of sliding of the sutures meanwhile in preventing potential tissue damage are basic requirements for clinical surgery, but these two sides are contradictory. Lowering the friction coefficient can make thread-to-tissue sliding and knot tying much easier. However, it results in difficulty in keeping up a knot. Tomita et al.[16,17] pointed out that silk sutures showed excellent knot security and low knot tie down resistance (the capacity of a knot to be slid down a strand[38]). He also demonstrated that the pullout resistance of a silk suture had two characteristics: high static resistance in the low-load region and relative low dynamic resistance. The former was concerned with knot security, and the latter was connected with sliding capacity. The result of withdrawal resistance (Figure 11) indicated that the thread-to-thread friction increased and the *D*-value dwindled for the M1 group. This phenomenon was caused by the increase in surface roughness and irregularity of the M1 group. However, the superficial friction significantly reduced but the *D*-value enlarged for the M2 group. These results are similar to monofilament sutures, because filling of antibacterial polymer into the interstices made the surface much smoother.

The stiffness of a suture material is closely related to its handling properties and knot security.[39] Some common views on bending stiffness of sutures have been achieved, such as braided sutures are more flexible than monofilament ones, coating always makes sutures stiffer, and the larger suture diameter increases its stiffness.[40] The bending stiffness of the the M1 group sutures is not remarkably increased compared with that of synthetic sutures, such as the 19.98 cN × mm^2 for polyamide (PA) and 14.89 cN × mm^2 for polypropylene (PP) monofilament sutures we tested. However, the bending stiffness of the M2 group increased sharply and gradually approached that of monofilament sutures, especially the bending stiffness of M2-3.

CONCLUSION

In this study, we prepared novel antibacterial braided silk sutures by using two different processing sequences with an LVFX-HCl and PCL antibacterial system. All prepared sutures showed ideal antibacterial efficacy against *S. aureus* and *E. coli* and could effectively prevent bacteria adherence. Slow drug release was realized by diffusion of drug in aqueous medium and the hydrolytic degradation of dosage. M1-2 samples showed acceptable cytotoxicity according to ISO 10993-5. Physical and handling properties of M1 group deteriorated slightly, while those of the M2 group changed significantly, after increase in more coatings. All novel sutures have alternative potential for production applications as high slow-release antibacterial silk suture materials. Considering the physical and handling characteristic requirements, sutures prepared with method 1 are proven suitable for clinical applications. However, more work is required to confirm the clinical safety and biocompatibility of the sutures *in vivo*.

AUTHOR INFORMATION

Corresponding Author

*E-mail: wanglu@dhu.edu.cn.

Notes

The authors declare no competing financial interest.

ACKNOWLEDGMENTS

This work was supported by the 111 project "Biomedical Textile Materials Science and Technology" (Grant B07024), the China Scholarship Council Fund (File No. 201406630047), and the Chinese Universities Undergraduate Innovative Fund (Grant No. DHU2012047). We gratefully acknowledge Nantong Horcon Medical Technology Co., Ltd., Haimen, China, for their kind supply of silk raw materials. We also express thanks for Xingyou Hu for his assistance of *in vitro* cytotoxicity test.

REFERENCES

(1) Mangram, A. J.; Horan, T. C.; Pearson, M. L.; Silver, L. C.; Jarvis, W. R. HICPAC. Guideline for Prevention of Surgical Site Infection, 1999. *Am. J. Infect. Control* **1999**, *27*, 97−134.

(2) Al-Niaimi, A. N.; Ahmed, M.; Burish, N.; Chackmakchy, S. A.; Seo, S.; Rose, S.; Hartenbach, E.; Kushner, D. M.; Safdar, N.; Rice, L.; Connor, J. Intensive Postoperative Glucose Control Reduces the Surgical Site Infection Rates in Gynecologic Oncology Patients. *Gynecol. Oncol.* **2015**, *136*, 71−76.

(3) Magill, S. S.; Edwards, J. R.; Bamberg, W.; Beldavs, Z. G.; Dumyati, G.; Kainer, M. A.; Lynfield, R.; Maloney, M.; McAllister-Hollod, L.; Nadle, J.; Ray, S. M.; Thompson, D. L.; Wilson, L. E.; Fridkin, S. K. Multistate Point-Prevalence Survey of Health Care-Associated Infections. *N. Engl. J. Med.* **2014**, *370*, 1198−1208.

(4) de Lissovoy, G.; Fraeman, K.; Hutchins, V.; Murphy, D.; Song, D.; Vaughn, B. B. Surgical Site Infection: Incidence and Impact on Hospital Utilization and Treatment Costs. *Am. J. Infect. Control* **2009**, *37*, 387−397.

(5) Ata, A.; Valerian, B. T.; Lee, E. C.; Bestle, S. L.; Elmendorf, S. L.; Stain, S. C. The Effect of Diabetes Mellitus on Surgical Site Infections after Colorectal and Noncolorectal General Surgical Operations. *Am. Surg.* **2010**, *76*, 697−702.

(6) Chang, W. K.; Srinivasa, S.; Morton, R.; Hill, A. G. Triclosan-Impregnated Sutures to Decrease Surgical Site Infections: Systematic Review and Meta-Analysis of Randomized Trials. *Ann. Surg.* **2012**, *255*, 854−859.

(7) Edmiston, C. E.; Seabrook, G. R.; Goheen, M. P.; Krepel, C. J.; Johnson, C. P.; Lewis, B. D.; Brown, K. R.; Towne, J. B. Bacterial Adherence to Surgical Sutures: Can Antibacterial-Coated Sutures Reduce the Risk of Microbial Contamination? *J. Am. Coll. Surg.* **2006**, *203*, 481−489.

(8) Alexander, J. W.; Solomkin, J. S.; Edwards, M. J. Updated Recommendations for Control of Surgical Site Infections. *Ann. Surg.* **2011**, *253*, 1082−1093.

(9) Elek, S. D.; Conen, P. E. The Virulence of *Staphylococcus Pyogenes* for Man-A Study of the Problems of Wound Infection. *Br. J. Exp. Pathol.* **1957**, *38*, 573−586.

(10) Yazdankhah, S. P.; Scheie, A. A.; Høiby, E. A.; Lunestad, B.; Heir, E.; Fotland, T. Ø.; Naterstad, K.; Kruse, H. Triclosan and Antimicrobial Resistance in Bacteria: An Overview. *Microb. Drug Resist.* **2006**, *12*, 83−90.

(11) Aiello, A. E.; Larson, E. L.; Levy, S. B. Consumer Antibacterial Soaps: Effective or Just Risky? *Clin. Infect. Dis.* **2007**, *45*, S137−S147.

DOI: 10.1021/acsami.5b06239
ACS Appl. Mater. Interfaces 2015, 7, 22394−22403

(12) Obermeier, A.; Schneider, J.; Wehner, S.; Matl, F. D.; Schieker, M.; von Eisenhart-Rothe, R.; Stemberger, A.; Burgkart, R. Novel High Efficient Coatings for Anti-Microbial Surgical Sutures Using Chlorhexidine in Fatty Acid Slow-Release Carrier Systems. *PLoS One* **2014**, *9*, e101426.
(13) Pethile, S.; Chen, X.; Hou, D.; Wang, L. Effect of Changing Coating Process Parameters in the Preparation of Antimicrobial-Coated Silk Sutures: An *In Vitro* Study. *Fibers Polym.* **2014**, *15*, 1589−1595.
(14) Viju, S.; Thilagavathi, G. Characterization of Tetracycline Hydrochloride Drug Incorporated Silk Sutures. *J. Text. Inst.* **2013**, *104*, 289−294.
(15) Janiga, P.; Elayarajah, B.; Rajendran, R.; Rammohan, R.; Venkatrajah, B.; Asa, S. Drug-Eluting Silk Sutures to Tetard Post-Operative Surgical Site Infections. *J. Ind. Text.* **2012**, *42*, 176−190.
(16) Tomita, N.; Tamai, S.; Ikeuchi, K.; Ikada, Y. Effects of Cross-Sectional Stress-Relaxation on Handling Characteristics of Suture Materials. *Bio-Med. Mater. Eng.* **1994**, *4*, 47−59.
(17) Tomita, N.; Tamai, S.; Morihara, T.; Ikeuchi, K.; Ikada, Y. Handling Characteristics of Braided Suture Materials for Tight Tying. *J. Appl. Biomater.* **1993**, *4*, 61−65.
(18) *The United States Pharmacopeia and The National Formulary*, USP 37-NF 32; The United States Pharmacopeial Convention: Rockville, MD, USA, 2014.
(19) Rothenburger, S.; Spangler, D.; Bhende, S.; Burkley, D. *In Vitro* Antimicrobial Evaluation of Coated VICRYL* Plus Antibacterial Suture (Coated Polyglactin 910 with Triclosan) Using Zone of Inhibition Assays. *Surg. Infect.* **2002**, *3*, s79−s87.
(20) Ming, X.; Rothenburger, S.; Yang, D. *In Vitro* Antibacterial Efficacy of MONOCRYL Plus Antibacterial Suture (Poliglecaprone 25 with Triclosan). *Surg. Infect.* **2007**, *8*, 201−208.
(21) Schneider, L. A.; Korber, A.; Grabbe, S.; Dissemond, J. Influence of pH on Wound-Healing: A New Perspective for Wound-Therapy? *Arch. Dermatol. Res.* **2007**, *298*, 413−420.
(22) *Biological Evaluation of Medical Devices- Part 5: Tests for In Vitro Cytotoxicity*, ISO/CD 10993-5:2009; International Organization for Standardization: Geneva, Switzerland, 2009.
(23) Chen, X.; Hou, D.; Tang, X.; Wang, L. Quantitative Physical and Handling Characteristics of Novel Antibacterial Braided Silk Suture Materials. *J. Mech. Behav. Biomed. Mater.* **2015**, *50*, 160−170.
(24) Osterberg, B. Enclosure of Bacteria Within Capillary Multifilament Sutures as Protection Against Leukocytes. *Acta Chir. Scand.* **1983**, *149*, 663−668.
(25) Hoogkamp-Korstanje, J. A. A. *In-Vitro* Activities of Ciprofloxacin, Levofloxacin, Lomefloxacin, Ofloxacin, Pefloxacin, Sparfloxacin and Trovafloxacin Against Gram-Positive and Gram-Negative Pathogens from Respiratory Tract Infections. *J. Antimicrob. Chemother.* **1997**, *40*, 427−431.
(26) Ming, X.; Rothenburger, S.; Nichols, M. M. *In Vivo* and *In Vitro* Antibacterial Efficacy of PDS Plus (Polidioxanone with Triclosan) Suture. *Surg. Infect.* **2008**, *9*, 451−457.
(27) Zurita, R.; Puiggalí, J.; Rodríguez-Galán, A. Triclosan Release from Coated Polyglycolide Threads. *Macromol. Biosci.* **2006**, *6*, 58−69.
(28) Phadtare, D.; Phadtare, G.; Barhate, N.; Singh, A. M. Extended Release Formulation of BCS Class I Drugs. *World J. Pharm. Pharm. Sci.* **2015**, *4*, 1676−1688.
(29) Higuchi, T. Rate of Release of Medicaments from Ointment Bases Containing Drugs in Suspension. *J. Pharm. Sci.* **1961**, *50*, 874−875.
(30) Woodruff, M. A.; Hutmacher, D. W. The Return of A Forgotten Polymer-Polycaprolactone in the 21st Century. *Prog. Polym. Sci.* **2010**, *35*, 1217−1256.
(31) Huang, X.; Brazel, C. S. On the Importance and Mechanisms of Burst Release in Matrix-Controlled Drug Delivery Systems. *J. Controlled Release* **2001**, *73*, 121−136.
(32) Kundu, S. C.; Kundu, B.; Talukdar, S.; Bano, S.; Nayak, S.; Kundu, J.; Mandal, B. B.; Bhardwaj, N.; Botlagunta, M.; Dash, B. C.; Acharya, C.; Ghosh, A. K. Nonmulberry Silk Biopolymers. *Biopolymers* **2012**, *97*, 455−467.
(33) Altman, G. H.; Diaz, F.; Jakuba, C.; Calabro, T.; Horan, R. L.; Chen, J.; Lu, H.; Richmond, J.; Kaplan, D. L. Silk-Based Biomaterials. *Biomaterials* **2003**, *24*, 401−416.
(34) Shen, G.; Hu, X.; Guan, G.; Wang, L. Surface Modification and Characterisation of Silk Fibroin Fabric Produced by the Layer-by-Layer Self-Assembly of Multilayer Alginate/Regenerated Silk Fibroin. *PLoS One* **2015**, *10*, e0124811.
(35) Mao, Z.; Wang, B.; Ma, L.; Gao, C.; Shen, J. The Influence of Polycaprolactone Coating on the Internalization and Cytotoxicity of Gold Nanoparticles. *Nanomedicine* **2007**, *3*, 215−223.
(36) Wutticharoenmongkol, P.; Sanchavanakit, N.; Pavasant, P.; Supaphol, P. Preparation and Characterization of Novel Bone Scaffolds Based on Electrospun Polycaprolactone Fibers Filled with Nanoparticles. *Macromol. Biosci.* **2006**, *6*, 70−77.
(37) Lowry, K. J.; Hamson, K. R.; Bear, L.; Peng, Y. B.; Calaluce, R.; Evans, M. L.; Anglen, J. O.; Allen, W. C. Polycaprolactone/Glass Bioabsorbable Implant in A Rabbit Humerus Fracture Model. *J. Biomed. Mater. Res.* **1997**, *36*, 536−541.
(38) Roby, M. S.; Kennedy, J. In *Biomaterials Science: An Introduction to Materials in Medicine*, 2nd ed.; Ratner, B. D., Hoffman, A. S., Schoen, F. J., Lemons, J. E., Eds.; Elsevier Academic Press: San Diego, CA, 2004; p 616.
(39) Chu, C. C.; Kizil, Z. Quantitative Evaluation of Stiffness of Commercial Suture Materials. *Surg., Gynecol. Obstet.* **1989**, *168*, 233−238.
(40) Chu, C. C. In *Biotextiles as Medical Implant*; King, M. W., Gupta, B. S., Guidoin, R., Eds.; Woodhead: Cambridge, U.K., 2013; pp 232−242.

DOI: 10.1021/acsami.5b06239
ACS Appl. Mater. Interfaces 2015, 7, 22394−22403